ISSN 1063-7826, Semiconductors, 2011, Vol. 45, No. 6, pp. 753–760. © Pleiades Publishing, Ltd., 2011.
Original Russian Text © V.P. Kladko, A.V. Kuchuk, N.V. Safryuk, V.F. Machulin, A.E. Belyaev, R.V. Konakova, B.S. Yavich, B.Ya. Ber, D.Yu. Kazantsev, 2011, published in Fizika i Tekhnika Poluprovodnikov, 2011, Vol. 45, No. 6, pp. 770–777.

Evolution of the Deformation State and Composition as a Result of Changes in the Number of Quantum Wells in Multilayered InGaN/GaN Structures

V. P. Kladko[a]^, A. V. Kuchuk[a], N. V. Safryuk[a], V. F. Machulin[a], A. E. Belyaev[a], R. V. Konakova[a], B. S. Yavich[b], B. Ya. Ber[c], and D. Yu. Kazantsev[c]

[a] *Lashkaryov Institute of Semiconductor Physics, National Academy of Sciences of Ukraine, Kyiv, 02028 Ukraine*
^e-mail: kladko@isp.kiev.ua
[b] *ZAO Svetlana-Optoelectronics, St. Petersburg, 194156 Russia*
[c] *Ioffe Physical Technical Institute, Russian Academy of Sciences, St. Petersburg, 194021 Russia*

Submitted November 11, 2010; accepted for publication November 23, 2010

Abstract—The methods of high-resolution X-ray diffraction have been used to study the multilayered structures in an $In_xGa_{1-x}N/GaN$ system grown by the method of metal–organic chemical-vapor deposition. A correlation between the strain state (relaxation) of the system, the indium content within quantum wells, the ratio of the barrier/well thicknesses, and the number of quantum wells in the active superlattice is established. It is shown that partial relaxation is observed even in a structure with one quantum well. The results we obtained indicate that the relaxation processes are bound to appreciably affect the optical characteristics of devices.

DOI: 10.1134/S1063782611060121

1. INTRODUCTION

Multilayered epitaxial quantum-dimensional structures based on InGaN/GaN solid solutions are widely used in fabrication of light-emitting diodes and laser diodes that emit in the visible and ultraviolet regions of spectrum [1]. Larger mismatches of lattice parameters are characteristic of layers of nitride structures; these mismatches give rise to strains that bring about high piezoelectric fields. In addition, a high density of dislocations, roughness of heteroboundaries, and fluctuations of composition are present in these layers. All these factors affect the optical properties of the structures under consideration. At present, there is a problem regarding growth of ternary solid solutions based on the III–N compounds, for example, $In_xGa_{1-x}N$ with a high content of indium ($x \geq 0.2$) [2]. It is known that an increase in the content of indium in such compounds brings about a degradation in their structural and optical characteristics.

The phase separation and surface segregation mainly of indium atoms represent another problem for this material [3]. It was shown by Bai et al. [4] that relaxation of strains sets in only for three-period structure, while it was established [5] that, at 18 superlattice (SL) periods, deterioration of crystallinity leads to complete degradation of the structure. The evolution of the composition and strains with the thickness of the well was studied previously [6–10]. At the same time, it was stated recently [11] that relaxation of stresses does not occur even with a larger number of quantum wells (QWs) in SL structures with small widths of QWs (1.5–2.5 nm) and moderate content of indium (<20%) in these structures.

One can compensate for the mismatch stresses and improve the crystallinity of heterostructures by growing intermediate buffer layers and SLs [12]. In the context of this, the study of the deformation state of such systems represents an urgent problem both in the technology of fabrication of the layers and in understanding of its effect on the luminescent properties of the structures. In order to optimize the process of fabrication of nitride heterostructures, it is necessary to accurately determine the relation between the initial fluxes of components and the parameters (thickness and composition) of a QW in the InGaN/GaN structures in relation to the growth conditions, which also represents an extremely important problem.

X-ray diffractometry is used to determine the structural parameters of multilayered systems; these parameters include the composition and thickness of separate layers, and also the sequence of their positions (the SL period). In addition, diffraction curves provide data on the abruptness of heteroboundaries (the presence of intermediate layers) and deformation of the layers, as well as on the composition and on the type of defects [13, 14].

In this study, we consider the issues of evolution of the deformation state and composition of an InGaN/GaN system in relation to the architecture of the active SL (the number of QWs) tuned to the radia-

tion wavelength close to 460 nm. We report the results of studying variations in the parameters of SL layers with high accuracy using a combination of methods of high-resolution X-ray diffractometry (HRXD).

2. EXPERIMENTAL

We performed X-ray structural studies of the samples that were obtained by metal–organic chemical-vapor deposition (MOCVD) and contained two periodic quantum-dimensional InGaN/GaN regions [13, 14]. We grew sequentially a "low-temperature" seeding GaN layer (with a thickness of 20 nm) and a buffer n-GaN layer (with a thickness of ~3.5 μm) on the surface of a (0001) sapphire substrate. In order to reduce the value of mismatch strains and the density of threading dislocations in the layers of the active region in an InGaN/GaN structure, we grew a five-period buffer InGaN(4 nm)/GaN (5 nm) SL with a relatively low indium content (~5%) in the InGaN QWs. The active region of the structure consisted of InGaN QWs (with a thickness of ~3 nm and with the nominal indium content ~12%) separated by GaN barriers with a thickness of ~9 nm. A p-GaN contact layer with a thickness of 0.1 μm was deposited on top of the active region. The studied samples differed in the number of QWs (periods) in the active region. The number of QWs was equal to five, three, and one in samples nos. 1208, 1226, and 1227, respectively.

With the aim of confirming the main parameters of the structures, we studied the distribution of indium over depth using a CAMECA IMS7f secondary-ion mass spectrometer. In order to study the depth distribution of components in structures, we used the primary Cs^+ ions and detected the secondary charged CsX^+ clusters (X = Ga, In). The impact energy of primary ions was chosen as equal to 1 keV (with the sample potential +2 kV) to improve the distribution over depth in the InGaN/GaN SL region. The depth of the etching crater was measured using an AMBIOS XP1 mechanical profilometer [15].

The X-ray structural studies of the samples were performed using a PANalytical X'Pert PRO MRD high-resolution diffractometer. In order to determine the structural parameters, we studied both the reciprocal-space maps (RSMs) and the diffraction-reflection curves (DRCs) measured in a high-resolution three-crystal configuration. Theoretical DRCs were calculated using the method of plane waves [16]; this method is well suited for studies of planar structures and is consistent with the Takagi–Topena method [17] (yields the same results). The wave vectors in the crystal were calculated previously; the results were reported in [18, 19].

Analysis of the dislocation structure of the SL layers was performed using the method described in [20, 21], while the deformed state was analyzed using the methods described in [22, 23]. We used the following parameters of the layers: for GaN: a = 3.1896 ± 0.0003 Å, c = 5.1855 ± 0.0002 Å, c/a = 1.6258 ± 0.0002, and p = 0.53 [24]; InN: a = 3.5378 ± 0.0001 Å, c = 5.7033 ± 0.0001 Å, c/a = 1.6121 ± 0.0001, and p = 0.49 [25].

3. RESULTS

A series of RSMs in the vicinity of the site $(\bar{1}\bar{1}24)$ for the InGaN/GaN structures under study are shown in Fig. 1. Analysis of asymmetric RSMs for the reciprocal-lattice sites the diffraction vector of which makes an angle φ with the normal to the surface allows one to obtain information on the degree of relaxation of heterostructures. For a completely stressed epitaxial structure, the intensity of coherent scattering from additional sites (centers of reflection from separate layers, thickness oscillations, and satellites of the superlattice) is distributed in the scattering plane parallel to the normal to the surface. For a completely relaxed structure, the sites are bound to be located along the diffraction vector. In the case of partial relaxation, the sites occupy intermediate positions. Thus, if the centers of the distribution of intensity corresponding to the layer and substrate are located along the normal to the surface, relaxation did not occur between them and the heteroboundary is coherent; in the opposite case, this is indicative of some degree of relaxation of the layer relative to the substrate.

In the case under consideration, the system of satellites is shifted with respect to the normal to the surface **n** (this normal is drawn from the site of the GaN buffer layer); this is indicative of partial relaxation of the SL relative to the buffer for all InGaN/GaN structures under study. It follows from the analysis of RSM that relaxation of SL is incomplete, since the sites of the SL are in an intermediate state between the direction of the diffraction vector **H** and normal **n** to the surface. It is worth noting that the shift of satellites relative to the normal **n** is observed even for the structure with a single QW; the degree of relaxation of the InGaN/GaN structures increases as the number of QWs is increased.

As can be seen from Fig. 1, the broad peaks at RSMs are observed both for the buffer GaN layer and for the InGaN/GaN SL. The large width of the peaks indicates that the layer contains defects (point defects, dislocations). It is known that epitaxial III–nitride layers grown on sapphire exhibit a high density of threading dislocations ($N_s \sim 10^{10}$ cm^{-2}), which bring about a pronounced broadening of diffraction reflections in the direction parallel to the surface [13, 14, 20–23]. The dislocation density ($N_s \sim 10^7$ cm^{-2}) in the active InGaN/GaN SL for the structures under study is lower by several orders of magnitude (see table), which is indicative of relaxation of elastic strains at the lower heteroboundary between the thick GaN buffer layer and the five-period InGaN/GaN SL buffer.

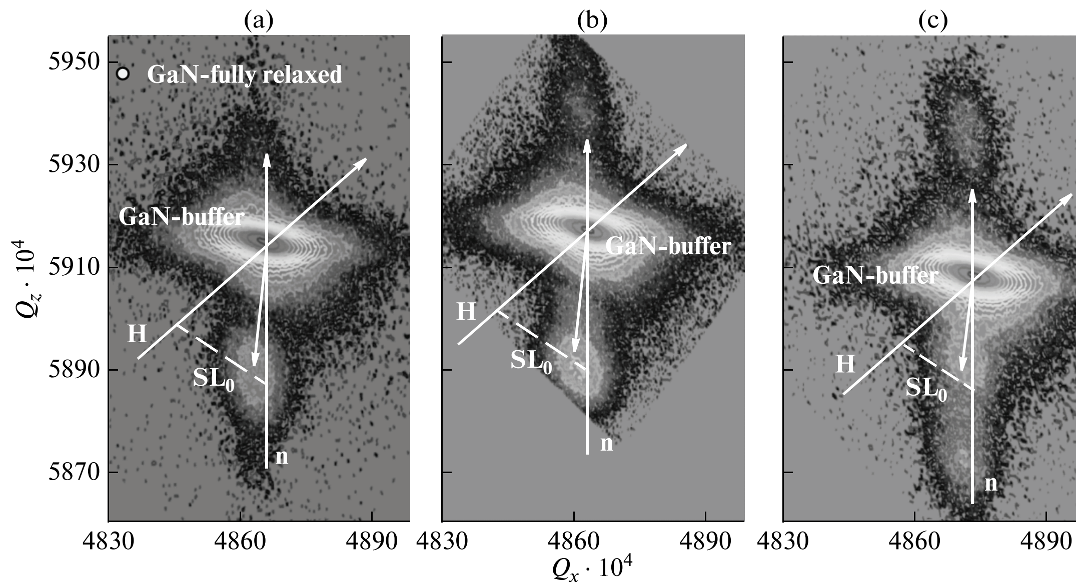

Fig. 1. RSMs in the vicinity of the site $(\bar{1}\bar{1}24)$ for the InGaN/GaN structures with (a) one, (b) three, and (c) five quantum wells. Q_z and Q_x are the coordinates in reciprocal space in units of $2\pi/\lambda$ in the directions perpendicular and parallel to the surface, respectively. **H** is the diffraction vector, **n** is the vector of the normal to the surface, and SL_0 is the position of the zero satellite related to the SL.

A more detailed analysis of parameters of the InGaN/GaN structures is carried out by simulation of experimental DRCs for the symmetric 0002 reflection (Fig. 2) using expressions of the dynamic theory with the parameters of partial relaxation (obtained from the RSM) taken into account. In Fig. 2, the sharp high-intensity peak corresponds to the 0002 reflection from the thick GaN buffer layer, while broader peaks (satellites) in the region of small and large angles correspond to the 0002 reflections from the active (SL_n) and buffer (SL_n^b) InGaN/GaN SL. The positions of the SL peaks depend on both the composition of the solid solution and the ratio between the layer thicknesses; it is noteworthy that, as the number of repetitions (quantum wells) is increased, the peaks related to SLs become sharper (Fig. 2). The presence of distinct satellites of high orders in DRCs is indicative of well-defined periodicity of the SL layers and, as can be seen from Fig. 2, these peaks broaden in comparison with calculated peaks. This broadening of satellites can be caused by spatial variations in the SL period (mixing and/or irregularities in the QWs) and/or fluctuations in the composition of the layers [26].

The distance $\Delta\theta$ between the main peaks of satellites designated as SL_{-1} and SL_0 corresponds to the one period of the SL ($T = t_w + t_b = |\gamma_h|\lambda/\sin(2\theta_B)\delta\theta$, where λ is the wavelength of the X-ray radiation, γ_h is the direction cosine of the diffracted beam, and t_w and

Technological (nominal) parameters and the parameters obtained from high-resolution X-ray diffractometry (HRXD) and secondary-ion mass spectrometry (SIMS) for the active InGaN/GaN SL

Sample	SL layers	t_{techn}/t_{exptl}	x_{techn}/x_{exptl}	T, nm		N_s, 10^7 cm^{-2}	R_{curv}, m
				HRXD	SIMS		
1227	GaN	–	12/9	–	–	8.37	6.8
	InGaN	3/3.0					
1226	GaN	6/7.7	12/14	11.5	13.5	6.00	6.6
	InGaN	3/3.8					
1208	GaN	6/7.9	12/12	11.8	14	7.37	7.9
	InGaN	3/3.9					

Note: t_{techn} and t_{exptl} are the nominal and experimental thicknesses of layers expressed in nanometers; x_{techn} and x_{exptl} are the nominal and experimental content of In in %.

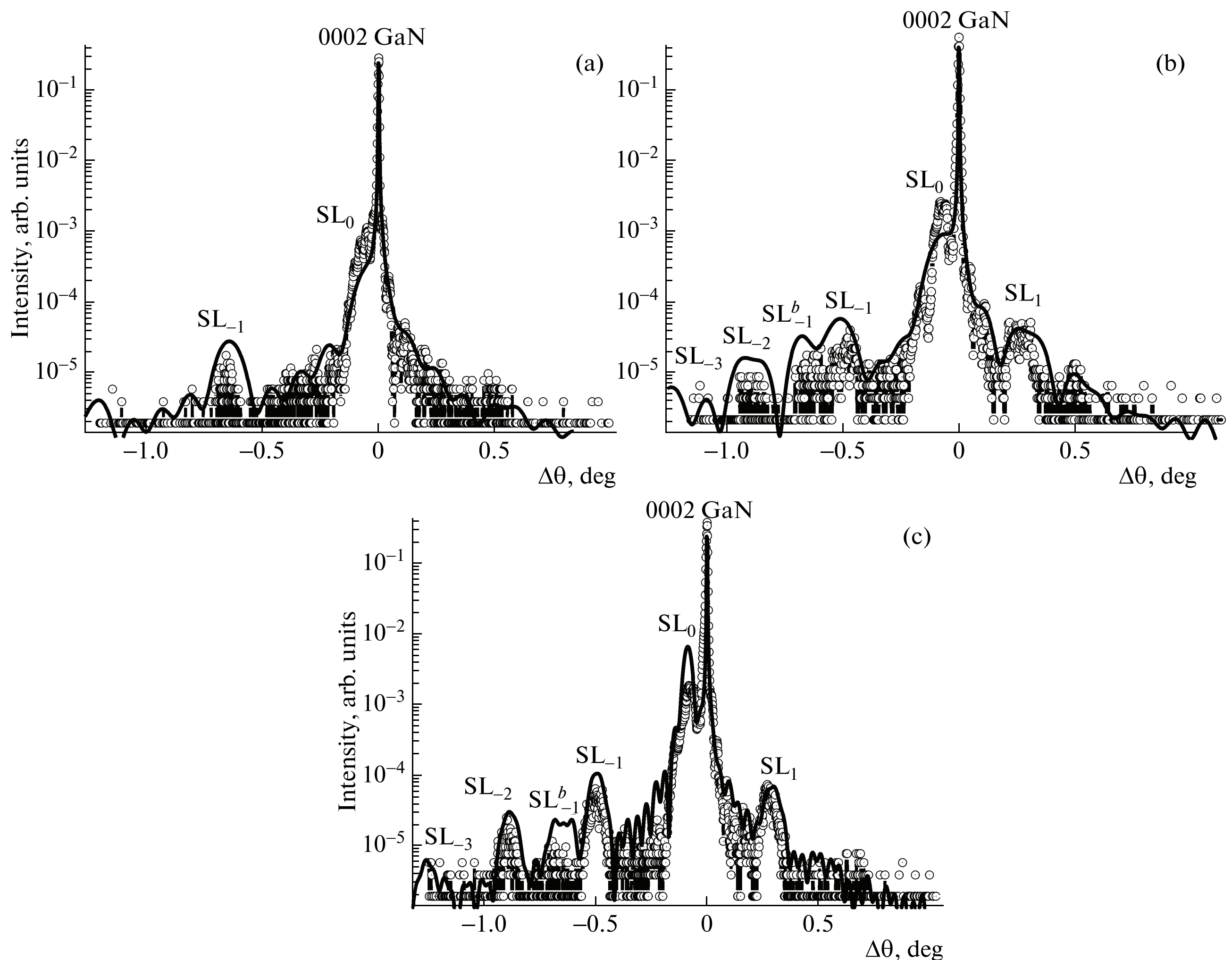

Fig. 2. The ω–2θ scans for the symmetric reflection 0002 from the InGaN/GaN structures with (a) one, (b) three, and (c) five quantum wells. Points represent experimental data, and the continuous line corresponds to the results of simulation. Designations SL_n correspond to satellites related to the active SL, and designations SL_n^b denote satellites related to the buffer SL.

t_b are the thicknesses of the QW and barrier layers), while faster interference oscillations are related to the total SL width.

The relative intensity of satellites was used to determine the ratio between the thicknesses and, then, also the composition of the solid solution.

The parameters of the active InGaN/GaN SL that were obtained from an RSM and refined using the procedure of fitting the calculated DRCs to the experimental curves [16, 27] are listed in the table and are shown in Fig. 3. The data on the SL period, which were derived from distribution profiles of the indium concentration over the depth in studied structures, are also listed in the table; the concentrations were measured by means of the method of secondary-ion mass spectroscopy (SIMS) [15]. The SL period correlates with the data of X-ray measurements within the experimental error of this method. The distribution profiles of the indium concentration over the depth of studied samples were measured by the SIMS method and are shown in Fig. 4.

As can be seen from the table and Fig. 3, a variation in the number of QWs in the active InGaN/GaN SL brings about appreciable changes in the degree of their strain, in the well/barrier thicknesses, and also in the indium concentration in the QW. It is worth noting here that the parameters of the buffer InGaN/GaN SL are identical for all structures: the QW width ~3.3 ± 0.02 nm, the barrier thickness ~4.5 ± 0.1 nm, and the In content in the QW ~4%.

As for the buffer GaN layer, the latter is found in a stressed state relative to the substrate and is partially relaxed; the degree of relaxation is approximately the same for all structures (Fig. 5), which is testified by the almost identical values of the curvature radius R_{curv} of the structures. This is supported by the fact that the thick III–nitride layers grown on sapphire almost completely relax during growth mainly due to disloca-

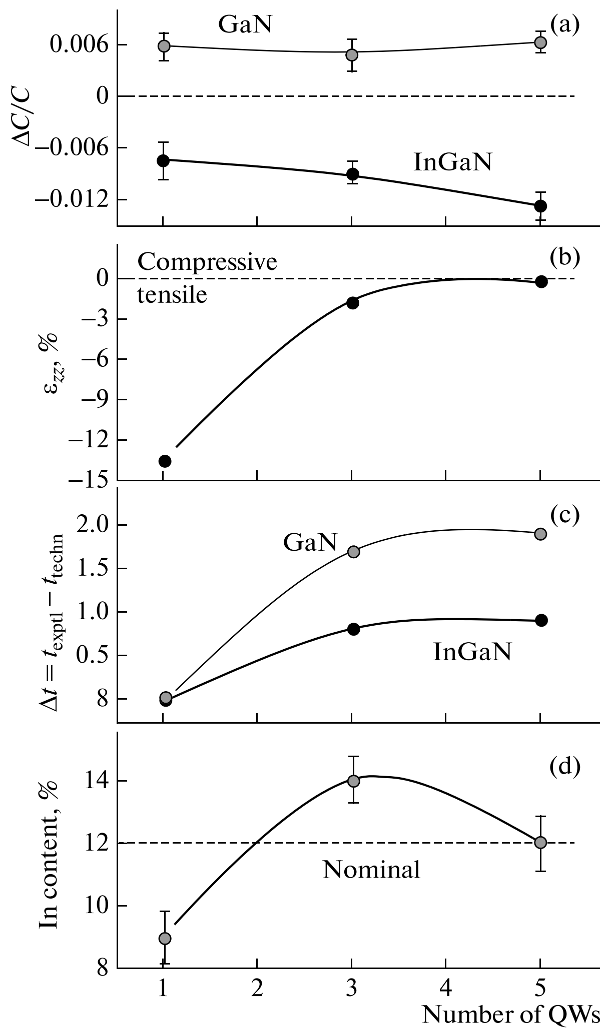

Fig. 3. Dependences on the number of quantum wells (QWs) in the active InGaN/GaN SL for (a) strains in the well/barrier layers, (b) strains averaged over the SL period and aligned along the growth direction [0001], (c) the difference between experimental and nominal thicknesses of the well/barrier layers, and (d) In content in the InGaN/GaN QW.

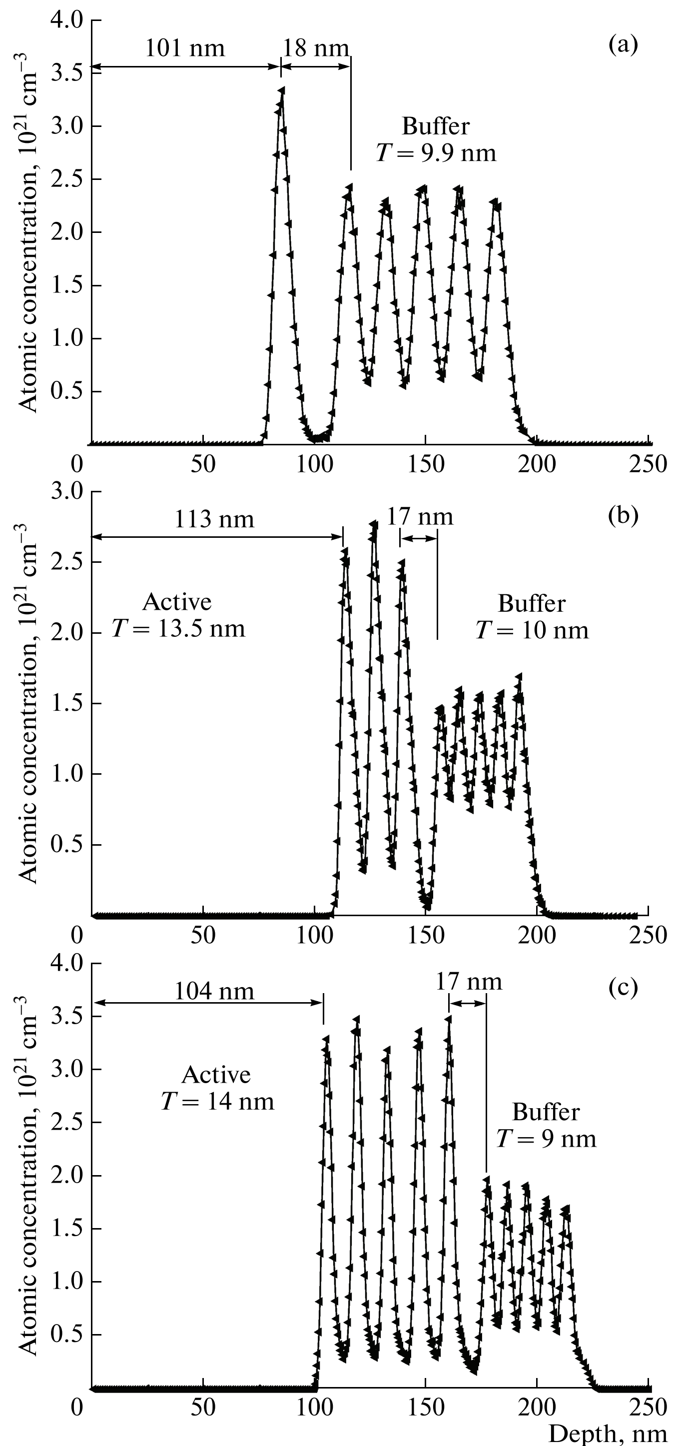

Fig. 4. The SIMS profiles of variation in the In concentration over the thickness of the samples with (a) one, (b) three, and (c) five QWs in the active region in the direction from the surface of the structures.

tions; the stresses observed in these layers at room temperature are mainly of thermal origin [22, 28].

However, although the process of relaxation of buffer layers has been studied to a large extent [20–23, 28], this problem remains under discussion for the SL layers. Here, besides classical mechanisms of relaxation due to cracks and misfit dislocations, the processes of thinning and thickening of one of the layers of SL during growth can occur; these processes represent additional channels for relaxation [29].

4. DISCUSSION

The active InGaN/GaN SL was grown on a buffer SL with a lower content of indium; in turn, the latter CL was formed on a partially relaxed GaN buffer layer. This and the consideration that the InGaN/GaN SLs under study exhibit relatively small thicknesses of the layers themselves and a small total thickness of the SL bring about an increase in the mismatch between lattices of two layers as the content of In in the QW is

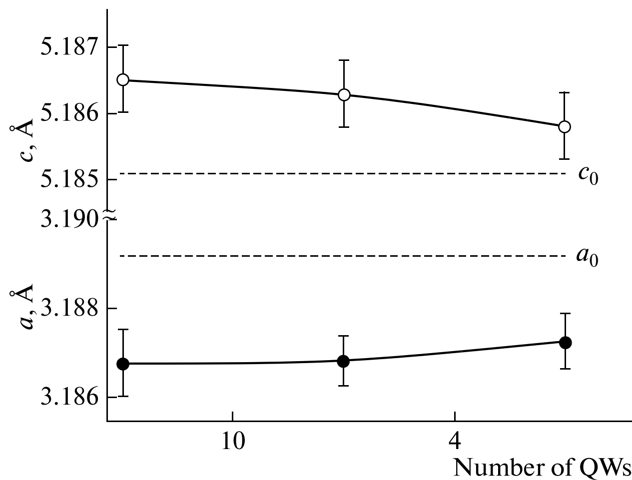

Fig. 5. Dependences of lattice constants in the GaN buffer layer on the number of quantum wells (QWs).

increased. Therefore, an SL can be characterized by two parameters of relaxation, i.e., relaxation of the SL as a complete unit in relation to the buffer layer and relaxation between separate SL layers.

Indeed, for all studied SLs, we observe partial relaxation at the lower heteroboundary, i.e., relief of stresses between the active SL in general and the buffer GaN layer due to the buffer SL. This is witnessed by the difference between parameters *a* of lattices of the buffer layer and the period-averaged active SL. Relaxation for structures with even a single QW, as can be seen from RSMs, indicates that all DLs relax at the lower boundary (a high density of dislocations) and then, as the number of QWs is increased, their crystal quality improves.

As can be seen from Fig. 3a, the GaN layers in the SL period are in a state of extension (the strain $\varepsilon_{GaN} > 0$), while the layers of the solid solution are in a state of compression (the strain $\varepsilon_{InGaN} < 0$) in the growth plane; this is observed for all studied structures. The tensile strain in the GaN layers is lower than compressive strains in the InGaN layers, which is mainly caused by thicknesses of the layers. In addition, the strain in the GaN barrier layers remains practically unchanged, whereas a monotonic increase in the strain is observed in the InGaN layers as the number of QWs in the active InGaN/GaN SL is increased. At the same time, the averaged value of strain in the direction of growth (ε_{zz}) drastically decreases in a single period of the active SL as the number of QWs is increased (Fig. 3b). Such behavior of strain in a period of the SL can be accounted for on the basis of the definition of the averaged parameters. The averaged values of strains (and also of other parameters) in a period were calculated using the following formula:

$$\varepsilon_{zz} = \frac{\varepsilon_1 t_1 + \varepsilon_2 t_2}{t_1 + t_2};$$

here, ε_1, t_1 and ε_2, t_2 are the average values of strains and thicknesses for the GaN and InGaN SLs, respectively [30]. The values of strains are determined from the formula $\varepsilon_{c(a)} = [c(a) - c_0(a_0)]/c_0(a_0)$, where $c(a)$ and $c_0(a_0)$ are the lattice parameters for nonrelaxed and relaxed structures, respectively. It can be seen that the average strain in a period of the SL heavily depends on the ratio of the thicknesses' well/barrier and on the lattice parameters of adjoining layers (composition of the well). Indeed, depending on the number of periods in the active SL, a different degree of deviation from specified thicknesses of the GaN and InGaN layers is observed (see Fig. 3c); variations in the composition of the InGaN QW can be seen from Fig. 3d.

A variation in the parameter $\Delta t = t_{exptl} - t_{techn}$, which represents the difference between the experimental and technological thicknesses of layers in a period of the active SL, is most likely caused by a difference in the strain state of SL, is most likely caused by the difference between the strain state for the SL and $InGaN/GaN/Al_2O_3(0001)$ used for determination of nominal growth rates and compositions. The InGaN layers in these samples had a thickness of ~100 nm and were almost completely relaxed. It follows from the data shown in Fig. 3c that, as the degree of the SL relaxation increases, the thicknesses of QWs in InGaN somewhat increase, whereas a difference between the thicknesses is not observed for structures with a single QW. An increase in the growth rate for the InGaN QW as the stresses in the substrate are reduced was observed by Johnson et al. [31]. Evidently, such behavior of layers' thicknesses brings about a variation in the strain state of the system, similarly to the effect for the GaN/AlN SL described by Kladko et al. [32]. However, additional studies are needed in order to interpret a relatively larger variation in the thickness of GaN barriers compared with the InGaN QWs.

As for the origin of the effect of an increase in the indium concentration with the number of periods in the SL (Fig. 3d), it was noted previously [11, 13] that the efficiency of incorporation of indium into the InGaN layers depends on the value of elastic stresses. It was predicted [11, 13] that incorporation of indium into the lattice is appreciably suppressed if there are stresses. Consequently, an increase in the indium concentration in a QW as the number of periods is increased can be attributed to relaxation of stresses in the system. Indeed, as a result of relaxation of stresses, the rates of growth of InGaN QW and In content in layers increase due to a decrease in the desorption time for In atoms from the surface and their capture by a growing layer. The results of simulation of X-ray spectra (the high-order satellites in SL are broadened in comparison with calculated values) can be accounted for by a variation in the In concentration from layer to layer, which is caused by the effects of In segregation at the growth surface.

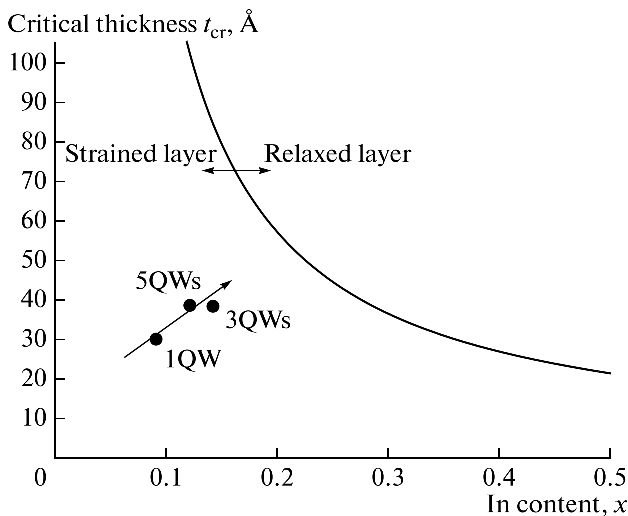

Fig. 6. The calculated dependence of the critical thickness of the layer (t_{cr}) for an $In_xGa_{1-x}N/GaN$ SL on the In content x.

In our opinion, the dependence of the parameter Δt (the rate of growth of the layers) and the In content on the number of QWs is caused by the effect of strain fields on the process of segregation of Ga(In) atoms in growing layers.

As can be seen from the table and Fig. 3, variation in the strain in the SL layer is not accompanied by significant changes in the dislocation density N_s and in the curvature radius R_{curv} of the structures; i.e., the SLs can relax differently at identical bending of the structures and identical dislocation density. This establishes that spontaneous variation in the thickness of the GaN and InGaN layers and variation in the QW composition represent additional channels for relaxation of stresses in the InGaN/GaN SL. Moreover, these processes, as well as defect formation, and, consequently, relaxation of stresses are interrelated. This is easily understood if we draw the dependence of critical thickness of the layer (t_{cr}) for $In_xGa_{1-x}N/GaN$ on the composition (x) and use the model suggested by Fisher et al. [33]. It can be seen from Fig. 6 that the SLs under study belong to the subcritical energy region where relaxation of mismatch stresses is excluded only due to dislocations. Indeed, the thicknesses of layers in the case under consideration are smaller than h_{cr} and relaxation of stresses in these layers due to elastic interaction between misfit dislocations seems to be impossible. Consequently, here, other relaxation channels are in effect, such as, for example, spontaneous variation in the thickness (composition).

We intentionally disregarded a detailed analysis of parameters of the buffer SL. It is worth noting that identical average parameters of the buffer SL for all structures suggest that, irrespective of the number QWs, the parameters of the first well in all structures are bound to be identical, the same as for the second, third, etc., wells.

5. CONCLUSIONS

Using the methods of X-ray diffraction, we determined the strained state of the active SL and its separate layers; the degree of relaxation; and the period, thicknesses of the layers, and the composition of an $In_xGa_{1-x}N$ solid solution.

It is established that, even at low concentrations of In in a QW, partial relaxation of multilayered structures occurs and affects the redistribution of indium in the layers.

It is shown that the processes of relaxation of stresses in multilayered structures set in even at an SL with a single quantum well. The degree of relaxation increases as the number of periods in the SL is increased. An increase in the degree of relaxation brings about an increase in the indium concentration in a QW. The latter increase is accompanied by variations in thicknesses of both wells and barriers.

We considered main channels of relaxation of the structures under study; these channels include dislocations in the layers and variations in the thickness of layers in the course of structures' growth. It is established that the structural properties of the SL are determined to a great extent by processes of inelastic relaxation of stresses, which, in turn, depend on the conditions of growth, in particular, on the temperature of growth of QWs and their thicknesses.

ACKNOWLEDGMENTS

This study was supported by the National Academy of Sciences of Ukraine within the framework of projects nos. 3.5.1.12, 2.2.13.2, and 3.5.1.30 (the state special scientific–technological program "Nanotechnology and Nanomaterials") and by the Ministry of Education and Science of Ukraine (project no. M90/2010).

REFERENCES

1. S. Nakamura and G. Fasol, *The Blue Laser Diode: GaN Based Light Emitters and Lasers* (Springer, Berlin, 1997).
2. F. K. Yam and Z. Hassan, Superlatt. Microstruct. **43**, 1 (2008).
3. R. Singh, D. Doppalapudi, T. D. Moustakasa, and L. T. Romano, Appl. Phys. Lett. **70**, 1089 (1997).
4. J. Bai, T. Wang, and S. Sakai, J. Appl. Phys. **90**, 1740 (2001).
5. S. Pereira, M. R. Correia, E. Pereira, K. P. O'Donnell, E. Alves, N. P. Barradas, A. D. Sequeira, N. Franco, L. M. Watson, and C. Liu, Phys. Status Solidi C **0**, 302 (2002).
6. A. Krost, J. Blasing, M. Lunenburger, H. Protzmann, and M. Heuken, Appl. Phys. Lett. **75**, 689 (1999).

7. J. H. Zhu, L. J. Wang, S. M. Zhang, H. Wang, D. G. Zhao, J. J. Zhu, Z. S. Liu, D. S. Jiang, Y. X. Qiu, and H. Yang, J. Phys. D: Appl. Phys. **42**, 235104 (2009).
8. A. M. Yong, C. B. Soh, X. H. Zhang, S. Y. Chow, and S. J. Chua, Thin Solid Films **515**, 4496 (2007).
9. S. Pereira, M. R. Correia, E. Pereira, K. P. O'Donnell, E. Alves, A. D. Sequeira, N. Franco, I. M. Watson, and C. J. Deatcher, Appl. Phys. Lett. **80**, 3913 (2002).
10. M.-I. Richard, M. J. Highland, T. T. Fister, A. Munkholm, J. Mei, S. K. Streiffer, C. Thompson, P. H. Fuoss, and G. B. Stephenson, Appl. Phys. Lett. **96**, 051911 (2010).
11. A. V. Sakharov, V. V. Lundin, E. E. Zavarin, M. A. Sinitsyn, A. E. Nikolaev, S. O. Usov, V. S. Sizov, G. A. Mikhailovskii, N. A. Cherkashin, M. Hytch, F. Hue, E. V. Yakovlev, A. V. Lobanova, and A. F. Tsatsul'nikov, Fiz. Tekh. Poluprovodn. **43**, 841 (2009) [Semiconductors **43**, 812 (2009)].
12. D. S. Lee, D. I. Florescu, D. Lu, J. C. Ramer, V. Merai, A. Parekh, M. J. Begarney, and E. A. Armour, Phys. Status Solidi A **201**, 2644 (2004).
13. V. V. Strel'chuk, V. P. Kladko, E. A. Avramenko, A. F. Kolomys, N. V. Safryuk, R. V. Konakova, B. S. Yavich, M. Ya. Valakh, V. F. Machulin, and A. E. Belyaev, Fiz. Tekh. Poluprovodn. **44**, 1236 (2010) [Semiconductors **44**, 1199 (2010)].
14. V. P. Kladko, A. V. Kuchuk, N. V. Safryuk, V. F. Machulin, A. E. Belyaev, R. V. Konakova, and B. S. Yavich, Semicond. Phys. Quant. Electron. Optoelectron. **13**, 1 (2010).
15. R. G. Wilson, F. A. Stevie, and C. W. Magee, *Secondary Ion Mass Spectrometry. A Practical Handbook for Depth Profiling and Bulk Impurity Analysis* (Wiley, 1989).
16. A. N. Efanov and V. P. Kladko, Metallofiz. Noveish. Tekhnol. **28**, 227 (2006).
17. A. Authier, *Dynamical Theory of X-Ray Diffraction* (Oxford Univ., New York, 2001).
18. Yu. P. Stetsko and S.-L. Chang, Acta Cryst. A **53**, 28 (1997).
19. O. M. Yefanov, V. P. Kladko, and V. F. Machulin, Ukr. J. Phys. **51**, 895 (2006).
20. V. P. Kladko, S. V. Chornenkii, A. V. Naumov, A. V. Komarov, M. Tacano, Yu. N. Sveshnikov, S. A. Vitusevich, and A. E. Belyaev, Fiz. Tekh. Poluprovodn. **40**, 1087 (2006) [Semiconductors **40**, 1060 (2006)].
21. V. P. Kladko, N. V. Safryuk, A. V. Kuchuk, A. E. Belyaev, and V. F. Machulin, Ukr. J. Phys. **54**, 1014 (2009).
22. V. P. Kladko, A. F. Kolomys, M. V. Slobodian, V. V. Strelchuk, V. G. Raycheva, A. E. Belyaev, S. S. Bukalov, H. Hardtdegen, V. A. Sydoruk, N. Klein, and S. A. Vitusevich, J. Appl. Phys. **105**, 063515 (2009).
23. V. P. Kladko, A. V. Kuchuk, N. V. Safryuk, V. E. Machulin, A. E. Belyaev, H. Hardtdegen, and S. A. Vitusevich, Appl. Phys. Lett. **95**, 031907 (2009).
24. M. Yamaguchi, T. Yagi, T. Sota, T. Deguchi, K. Shimada, and S. Nakamura, J. Appl. Phys. **85**, 8502 (1999).
25. W. Paszkowicz, Powder Diffract. **14**, 258 (1999).
26. A. T. Cheng, Y. K. Sua, and W. C. Lai, J. Cryst. Growth **298**, 508 (2007).
27. V. P. Kladko, L. I. Datsenko, J. Bak-Misiuk, S. I. Olikhovskii, V. F. Machulin, I. V. Prokopenko, V. B. Molodkin, and Z. V. Maksimenko, J. Phys. D: Appl. Phys. **34**, A87 (2001).
28. V. V. Ratnikov, R. N. Kyutt, T. V. Shubina, T. Pashkova, and B. Monemar, J. Appl. Phys. **88**, 6252 (2000).
29. P. K. Kandaswamy, C. Bougerol, D. Jalabert, P. Ruterana, and E. Monroy, J. Appl. Phys. **106**, 013526 (2009).
30. Yu. I. Mazur, Zh. M. Wang, G. J. Salamo, V. V. Strelchuk, V. P. Kladko, V. F. Machulin, M. Ya. Valakh, and M. O. Manasreh, J. Appl. Phys. **99**, 023517 (2006).
31. M. C. Johnson, E. D. Bourret-Courchesne, J. Wu, Z. Liliental-Weber, D. N. Zakharov, R. J. Jorgenson, T. B. Ng, D. E. McCready, and J. R. Williams, J. Appl. Phys. **96**, 1381 (2004).
32. V. P. Kladko, A. V. Kuchuk, N. V. Safryuk, V. F. Machulin, P. M. Lytvyn, V. G. Raicheva, A. E. Belyaev, Yu. I. Mazur, E. A. DeCuir, Jr., M. E. Ware, and G. J. Salamo, J. Phys. D: Appl. Phys. **44**, 025403 (2011).
33. A. Fisher, H. Kuhne, and H. Richter, Phys. Rev. Lett. **73**, 2712 (1994).

Translated by A. Spitsyn

SPELL: OK